Vol. 91 No. 4 pp. 1363–1379 ACTA GEOLOGICA SINICA (English Edition) Aug. 2017

Genesis of Dolomite from $Ma5^5$–$Ma5^{10}$ Sub-members of the Ordovician Majiagou Formation in the Jingxi Area in the Ordos Basin

LIU Jingdong[1, 2, *], JIANG Youlu[1], LIU Xinshe[3], YANG Zhiwei[4], HOU Xiangdong[3], ZHU Rongwei[5], WEN Caixia[3] and WANG Feiyan[3]

1 *School of Geosciences, China University of Petroleum, Qingdao 266580, China*
2 *State Key Laboratory of Petroleum Resources and Prospecting, China University of Petroleum, Beijing 102249, China*
3 *Research Institute of Exploration & Development, Changqing Oilfield Company, PetroChina, Xi'an 710018, China*
4 *Marine Oil Production Plant, Sinopec Shengli Oilfield, Dongying 257000, China*
5 *Key Laboratory of Marginal Sea Geology, South China Sea Institute of Oceanology, Chinese Academy of Science, Guangzhou 510301, China*

Abstract: We clarified three stages of dolomitization and secondary changes by studying the petrology and geochemistry characteristics of dolomite from the $Ma5^5$–$Ma5^{10}$ sub-members of the Ordovician Majiagou Formation in the Jingxi area in the Ordos Basin: (1) Syngenetic microbial dolomitization is characterized by formation of dolomite with a mainly micrite structure and horse tooth-shape dolomite cements. (2) Seepage reflux dolomitization during the penecontemporaneous period superposed adjustment functions such as recrystallization and stabilization in the middle-deep burial stage, forming dolomites mainly consisting of micro crystal and powder crystal structure. (3) Powder dolomite, fine dolomite, and medium-coarse crystalline dolomite formed in pores and fractures in the middle-deep burial stage. The secondary concussive transgression-regression under a regressive background is an important condition for the occurrence of many stages of dolomitization in the study area. The basin was an occlusive epicontinental sea environment in the Ma5 member of the Ordovician Majiagou Formation sedimentary period. In the sediments, sulfate content was high, which is conducive to the preservation of microbial activity and microbial dolomitization. Micritic dolomite formed by microbial dolomitization provides good migration pathways for seepage reflux dolomitization. Affected by evaporation seawater with increased Mg/Ca ratio, seepage reflux dolomitization was widely developed and formed large-scale dolomite, and underwater uplifts and slopes are favorable areas for dolomite. In the middle-deep burial stage, dolomitizing fluid in the stratum recrystallized or stabilized the previous dolomite and formed a small amount of euhedral dolomite in the pores and fractures.

Key words: Ordos Basin, Ordovician, genesis of dolomite, microbial dolomitization, seepage reflux dolomitization, burial dolomitization

1 Introduction

Lower Paleozoic Ordovician rock in the Ordos Basin has long been an important oil and gas exploration layer. Previous exploration and studies of Ordovician natural gas in the basin mostly concentrated on the solution pore reservoir of weathering crust in the $Ma5^1$–$Ma5^4$ sub-members of the Ordovician Majiagou Formation in the Jingbian Gas Field (Yang Hua and Bao Hongping, 2011). The new field in the form of a dolomite reservoir from the $Ma5^5$–$Ma5^{10}$ sub-members of the Ordovican Majiagou Formation was discovered in the Jingxi area, forming gas reserves of nearly 1000×10^8 m^3. This opened up a new prospect for lower Paleozoic Ordovician gas exploration in the Ordos Basin (Yang Hua et al., 2013).

The main reservoir pore space of dolomite in the study region is intercrystal pore and intercrystal dissolved pore. Therefore, dolomitization is crucial for the formation of

* Corresponding author. E-mail: ljd840911@126.com

© 2017 Geological Society of China

this kind of reservoir. As for dolomite from the Majiagou Formation in the Ordos Basin, many scholars have conducted studies and proposed different dolomitization models, such as penecontemporaneous dolomitization (Zhao Junxing et al., 2005; Huang Qingyu et al., 2010; Huang Zhengliang et al., 2011; Su Zhongtang et al., 2011, 2013), seepage reflux dolomitization (Huang Qingyu et al., 2010; Huang Zhengliang et al., 2011), mixed water dolomitization (Zhao Junxing et al., 2005; Bi Shengyu et al., 2005; Huang Zhengliang et al., 2011), burial dolomitization (Zhang Yongsheng, 2000; Bi Shengyu et al., 2005; Wang Baoquan et al., 2009; Huang Qingyu et al., 2010; Huang Zhengliang et al., 2011; Zhao Weiwei and Wang Baoqing, 2011; Su Zhongtang et al., 2011, 2013), hydrothermal dolomitization (Yao Jingli et al., 2009; Huang Qingyu et al., 2010; Huang Zhengliang et al., 2011), and microbial dolomitization (Fu Jinhua et al., 2011; Yang Hua et al., 2012). Scholars have researched Ma5 member dolomites of the Ordovician Majiagou Formation in the Jingxi area in recent years and have proposed different dolomitization patterns, such as penecontemporaneous dolomitization (Yu Zhou et al., 2012; Chen Hongde et al., 2013), seepage reflux dolomitization (Huang Zhengliang et al., 2012, 2014; He et al., 2014), mixed water dolomitization (Yang Hua and Bao Hongping, 2011; Fu Jinhua et al., 2011; Shi Baohong et al., 2013; Huang Zhengliang et al., 2014), and burial dolomitization (Chen Hongde et al., 2013; He et al., 2014). There is not yet a consensus on dolomitization of Ordovician layers in the Ordos Basin and the Ma5 member of the Ordovician Majiagou Formation in the Jingxi area. Compared to previous research, it has been found that the various dolomitization mechanisms in the Ordos Basin are closely related to the complexity of dolomite genesis in different locations. These findings are also influenced by data richness in the study area and differences in research degrees. Dolomitization requires two main conditions: a sufficient Mg^{2+} source and a migration mechanism to transport Mg^{2+} to the dolomitization location.

We used petrography data, including core observation, cast thin sections, scanning electron microscopy (SEM), and cathodoluminescence, from 20 wells in the Jingxi area of the Ordos Basin, to analyze dolomite type and the macroscopic distribution of $Ma5^5$–$Ma5^{10}$ sub-members of the Ordovician Majiagou Formation. We also analyzed geochemical characteristics such as crystal order degree, elements, isotopes, and fluid inclusions from the point of view of the genetic mechanism of dolomite. We discussed dolomitization fluid properties and fluid source, established dolomitization patterns, and analyzed the distribution range of dolomitization in each stage and its impact on reservoir. This should provide more bases for studying dolomitization and predicting Ordovician dolomite reservoir in the Ordos Basin.

2 Geological Settings

Located in the western part of the North China Plate, the Ordos Basin extends across Shaanxi, Gansu, Ningxia, Inner Mongolia, and Shanxi provinces, covering an area of 37×10^4 km^2 (Chen Hongde et al., 2013). The study area is west of the Jingbian area in the center of the basin (Fig. 1). During the early Paleozoic the area was affected by the Qinqi Trough on the southern margin and the Helan aulacogen on the western margin, forming an "L" type ancient uplift on the southwestern margin of the basin (known as the "Central Ancient Uplift"). The Central Ancient Uplift separated the basin into two sedimentary systems, the western Qilian Sea sedimentary system, which is dominated by a platform-margin slope environment, and the eastern North China Sea sedimentary system, which is dominated by an epicontinental sea environment (Hou Fanghao et al., 2003; Yang Hua and Bao Hongping, 2011; Chen Hongde et al., 2013). It was dry and hot in the eastern portion of the Central Ancient Uplift during the sedimentary period of the Ma5 member of the Ordovician Majiagou Formation. It was a regression environment as a whole, but a secondary concussive transgression-regression occurred under the large regressive background. The concussive transgression-regression environment influenced the development of interbedded deposition of gypsum-bearing carbonate in the eastern part of the Central Ancient Uplift (Fig. 2). There was a short-term transgressive hemicycle during the $Ma5^5$, $Ma5^7$, and $Ma5^9$ sub-members sedimentary periods. The development of sedimentary facies was affected by paleogeomorphological factors and characterized by zonal distribution around the eastern depression area of the basin. The following subfacies developed sequentially from west to east: Huanlong dolomite tidal subfacies, Jingxi platform plateau subfacies, Jingbian gentle slope subfacies, and eastern depression subfacies (Yang Hua and Bao Hongping, 2011). The Jingxi area mainly includes Huanlong dolomite tidal subfacies and Jingxi platform plateau subfacies, where dolomite, calcite-dolomite, and argillaceous dolomite were developed and intercalated by small amounts of gypsum-bearing dolomite locally. It was a short-term regressive hemicycle during the $Ma5^6$, $Ma5^8$, $Ma5^{10}$, and $Ma5^1$–$Ma5^4$ sub-members sedimentary periods. The framework of lithofacies and paleogeography was similar to that of the short-term transgressive hemicycle. The following subfacies developed sequentially from west to east: gypsum-bearing dolomite

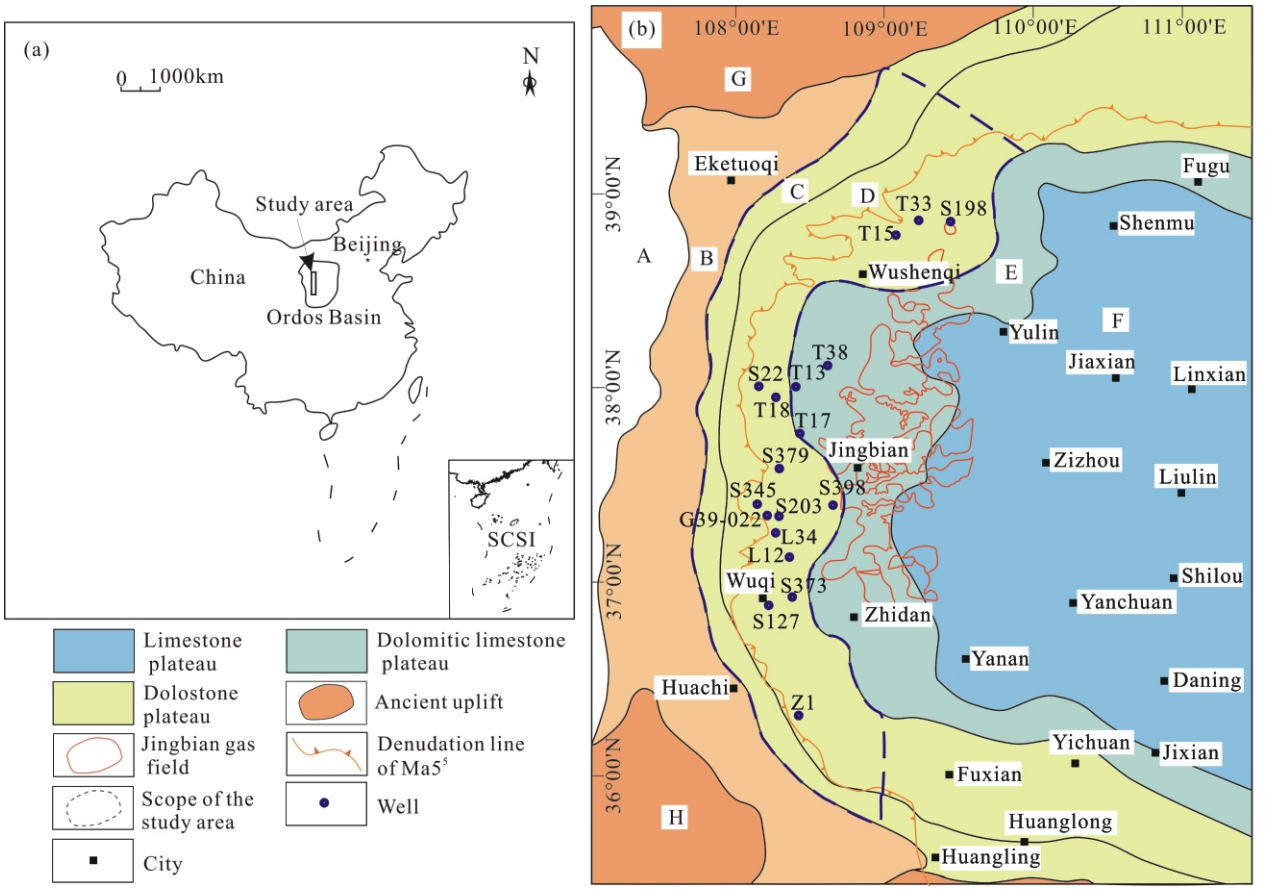

Fig. 1. The location of the study area and the sedimentary facies of the eastern portion of the Central Ancient Uplift in the Ordos Basin in the Ma5 deposition period.

tidal subfacies, gypsum-bearing dolomitic gentle slope subfacies, basin margin gentle slope subfacies, and salt rock basin subfacies. The Jingxi area mainly includes gypsum-bearing dolomite tidal subfacies and gypsum-bearing dolomitic gentle slope subfacies. Their rock types are similar to that of the $Ma5^6$, $Ma5^7$, and $Ma5^9$ sub-members, but are intercalated by more gypsum-bearing dolomite.

Caledonian orogeny after the Majiagou sedimentary period resulted in the overall uplift of the basin and weathering and erosion for more than 150 million years (Su Zhongtang et al., 2008, 2011). Erosion was particularly severe in the study area because it was located near the Central Ancient Uplift, thus upper Ordovician–lower Carboniferous layers were absent on the whole. The basin gradually transformed from an epicontinental basin to an intra-continental depression basin in the late Carboniferous. A coal-bearing clastic rock formation was deposited in the study area and contacted the underlying Majiagou Formation unconformably.

3 Samples and Methods

Nineteen dolomite samples and one pore space-filled dolomite sample were collected in this study. The samples are from the $Ma5^5$–$Ma5^{10}$ sub-members of the Ordovician Majiagou Formation and were collected from a depth range of 3043.3–4118.35 m. Casting thin sections, cathodoluminescence thin sections, and fluid inclusion thin sections were produced by the Experimental Center of the Academy of Science, China University of Geosciences (Beijing). Cathodoluminescence and fluid inclusion analysis were conducted at the Key Laboratory of Reservoir Geology, Shandong Province, China University of Petroleum (East China). The instrument for cathodoluminescence analysis was an ELM3R2L cathodoluminescence instrument. The instrument for fluid inclusion analysis was a ZEISS AXIO Imager D1m digital polarizing microscope and a Linkam THMS600 type hot and cold stage. The homogenization temperature test precision was ±1°C. Order degree and SEM analyses were conducted at the State Key Laboratory of Heavy Oil, China University of Petroleum (East China). The

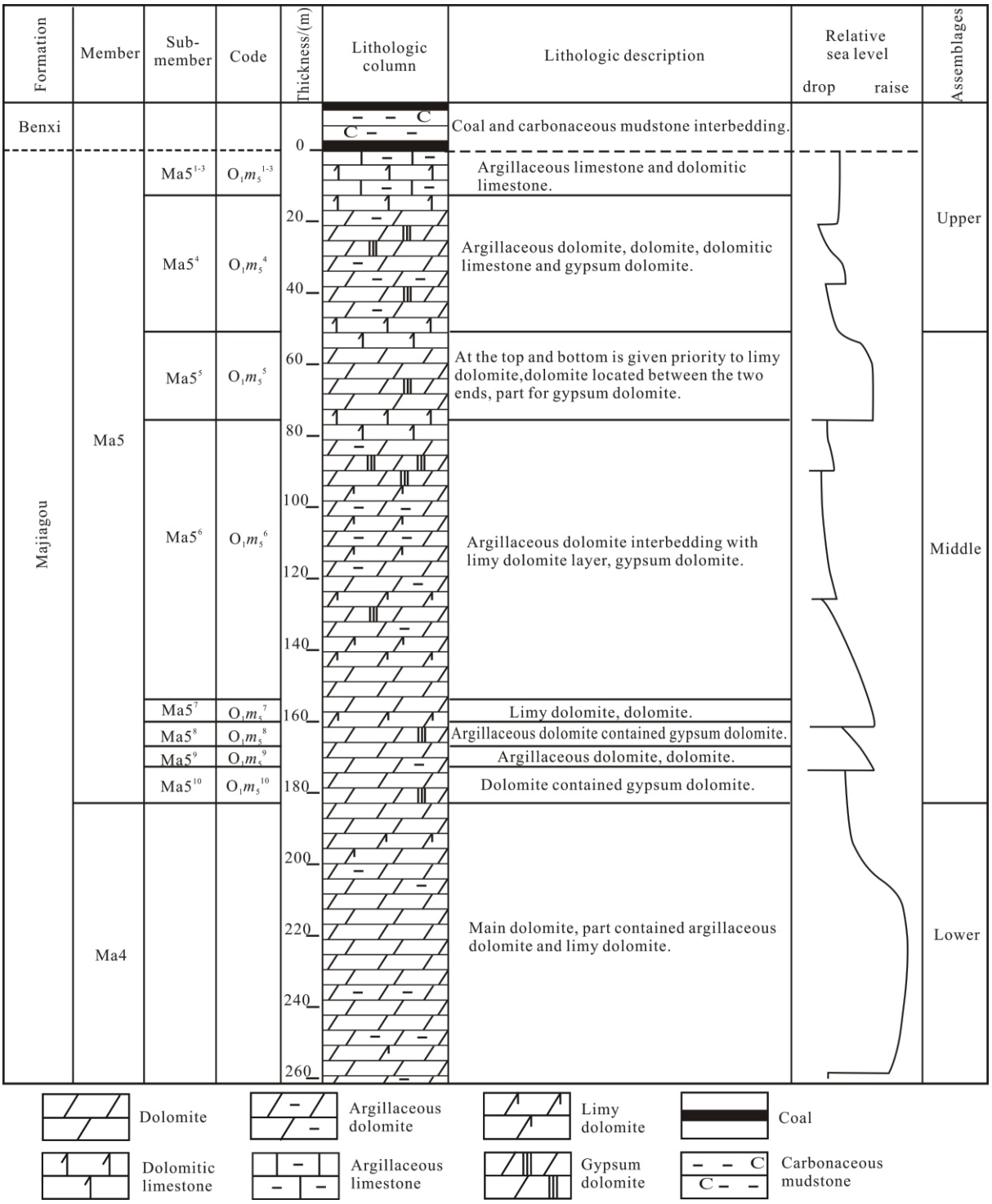

Fig. 2. Comprehensive stratigraphic column from Ma4 member to the Benxi Formation in the Jingxi area.

instrument for order degree analysis was a Model D/max-2500 X-ray diffractometer. The instrument for SEM analysis was a Model S-4800 high resolution cold field emission scanning electron microscope.

Analyses of $\delta^{13}C$ and $\delta^{18}O$ isotopes were conducted by the Rock Sample Preparation and Analysis Laboratory and Stable Isotope Analysis Laboratory, Institute of Geology and Geophysics of Chinese Academy of Sciences. The instrument for elemental analysis was a Model XRF-1500 X-ray fluorescence spectrometer, with an analysis error less than 0.1%. The instrument for $\delta^{13}C$ and $\delta^{18}O$ analysis was a Model MAT-253 stable isotope ratio mass spectrometer, with an analysis error less than 0.2‰.

Analysis of $^{87}Sr/^{86}Sr$ was conducted at the State Key Laboratory of Metallogenic Mechanism of Endogenic Metallic Ore Deposits, Nanjing University. The

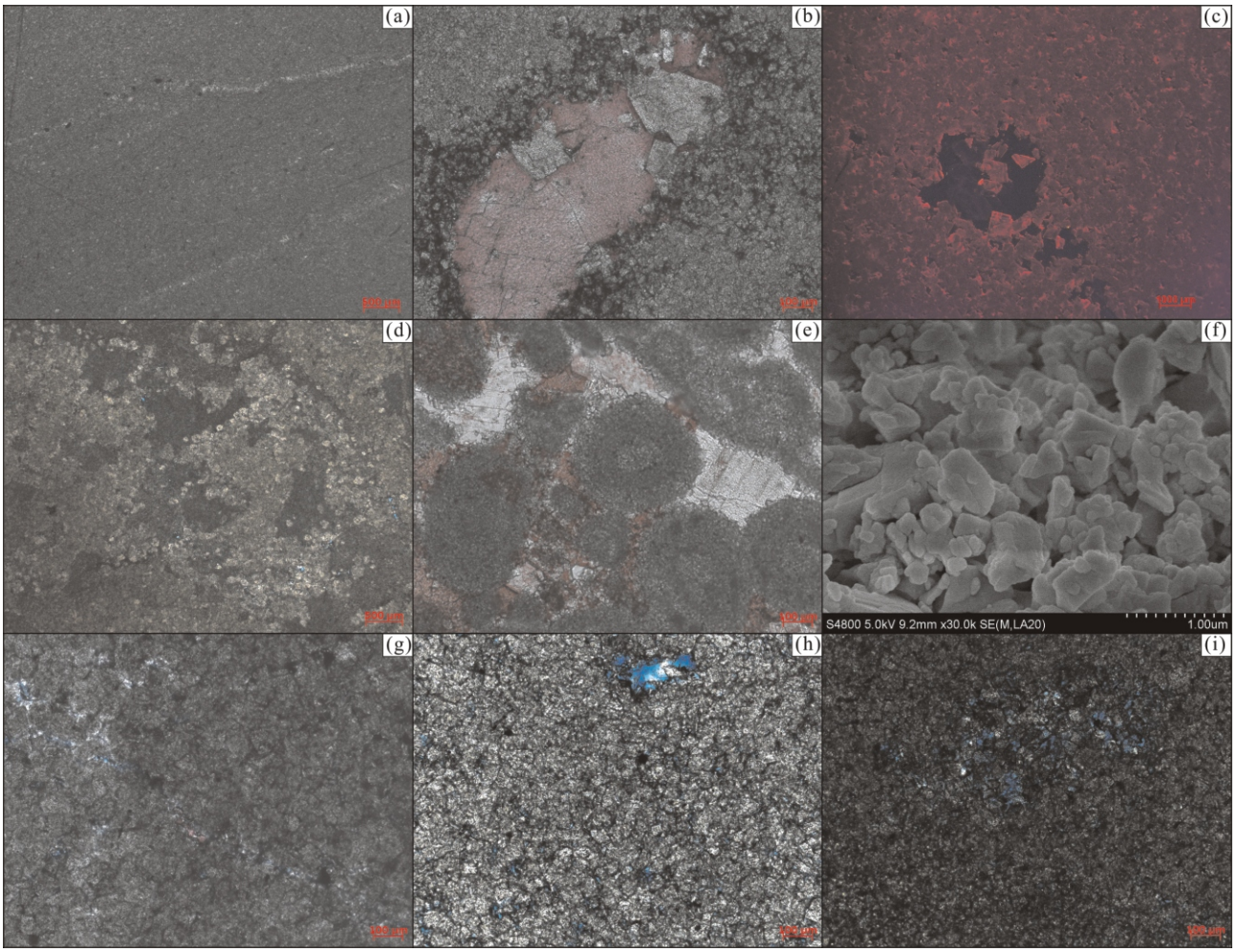

Fig. 3. Types of dolomite of the $Ma5^5$–$Ma5^{10}$ sub-members of the Ordovician Majiagou Formation in the Jingxi area.
(a), Lamina micritic dolomite (Well Z1, $Ma5^5$, 3881.32 m), plane-polarized light (PPL); (b), Micritic and microcrystal dolomite (Well T17, $Ma5^7$, 3744.84 m), clean fine dolomite filling in solution pores, PPL; (c), Powder dolomite emits dim light overall, part of margins of dolomite emit bright red light, dolomite in pores emits bright and dim zonal light (Well S203, $Ma5^5$, 3921.09 m), cathodoluminescence (CL); (d), Clot micritic and microcrystal dolomite, sparry dolomite intercalated among clots (Well T10, $Ma5^5$, 3706.44 m), PPL; (e), Intergranular dolomite (Well T17, $Ma5^6$, 3677.98 m), dolomite cements distribute as two generations, the first generation is horse teeth-shaped dolomite around margins of particles, the second generation is massive dolomite in intergranular pores with significant recrystallization, dedolomitization occurred in later stages locally or calcite cementation occurred in residual pores, PPL; (f), Spherical or short rod-like dolomite under SEM with a mostly aggregate distribution, (Well Z1, $Ma5^5$, 3886.8 m), scanning electron microscope (SEM); (g), Powder dolomite (Well S127, $Ma5^5$, 4119.59 m), PPL; (h), Powder dolomite (Well S345, $Ma5^5$, 3979.74 m), PPL; (i), Microcrystal and powder dolomite (Well S203, $Ma5^5$, 3921.09 m), PPL.

instrument was a NEPTUNE Plus multi-collector plasma mass spectrometer. The $^{87}Sr/^{86}Sr$ value of the strontium isotope standard sample obtained from repeated analysis was 0.710274±0.000005.

4 Results

4.1 Rock types and distributions

Based on dolomite microstructure, crystal form, crystal size, and cathodoluminescent characteristics (Fig. 3), we divide dolomites in the study area into three categories: ① Micritic and microcrystal dolomite with crystal sizes less than 0.01 mm. Part of crystal forms are spherical or short rod-like, and have laminated structure, algae bond, or clot structure, with sparry dolomite intercalated among algae bond framework, or clots. Sand cutting or metasomatic residual texture occurs. Cathodoluminescence intensity is weak and dolomites usually emit dim red light or no light. ② Powder dolomite (including intergranular dolomite cement) with crystal sizes between 0.01 and 0.05 mm. Crystal form is mainly straight plane and subhedral, with some that are non-straight plane and anhedral. It has laminated structure, and metasomatic residual texture often occurs. Two generations of cementation occurred in intergranular dolomite. The early generation was a horse tooth-like rim and the crystal form of the later generation was not obvious, with filled intergranular pores with lumpy structure revealing intense recrystallization. Cathodoluminescence intensity is similar to that of micritic dolomite on the whole, but many dolomite edges

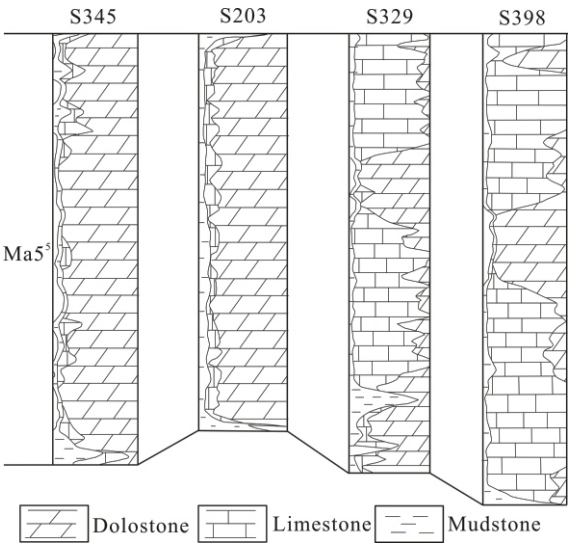

Fig. 4. Variation of dolomite content in the $Ma5^5$ sub-member in the Jingxi area in the EW direction.

reflect bright red. ③ Powder, fine, medium, and coarse dolomite in pores and fractures, with crystal sizes mostly between 0.01 and 0.25 mm and up to 1.0 mm. Dolomite crystals are cleaner and usually emit bright and dim zonal light under cathodoluminescence.

As for the dolomite categories of the types in our study, the $Ma5^5$ sub-members are mainly powder dolomite and microcrystal dolomite. $Ma5^6$–$Ma5^{10}$ sub-members are mainly powder dolomite, micritic, and microcrystal dolomite. Fig. 4 shows each sub-member, from west to east in the plane, with a gradual transition from powder dolomite to microcrystal, fine dolomite, or micritic and microcrystal dolomite, from entire dolomitization to partial dolomitization with decreasing dolomite content (Fig. 4).

4.2 Order degree of dolomite

Table 1 shows the order degree of dolomite from the $Ma5^5$–$Ma5^{10}$ sub-members of the Ordovician Majiagou Formation. In the study area, the order degree is 0.710–0.876, with an average of 0.791, indicating relatively small dispersion. The order degree of power dolomite in the $Ma5^{10}$ sub-members is relatively large (0.876). The order degree of microcrystal dolomite in the $Ma5^5$ sub-members (average 0.746) is lower than power dolomite, whereas micritic dolomite shows a greater order degree (0.799). The order degree of dolomite increases with burial depth as a whole except for a few individual samples. These characteristics reflect that the dolomite was formed in a generally similar diagenesis environment and that burial depth has some influence on order degree.

4.3 Element composition and carbon, oxygen, and strontium isotopes of dolomite

4.3.1 Element composition

Table 2 shows elemental analysis results of dolomite. For country rock dolomite of the $Ma5^5$–$Ma5^{10}$ sub-members, the representatives of terrigenous debris of SiO_2, TiO_2, and Al_2O_3 content vary greatly. SiO_2 content ranges from 0.25% to 2.91%, with an average of 1.41%, TiO_2 content ranges from 0.0048% to 0.0383%, with an average of 0.0156%, and Al_2O_3 content ranges from 0.05% to 0.67%, with an average of 0.26%. TFe_2O_3 content, which is representative of depositional environment or diagenesis, is generally less than 0.5%. It ranges from 0.18% to 0.55%, with an average of 0.30%. MnO content is between 0.0078% and 0.0404%, with an average of 0.0252%. Low Mn content may be the reason for low background value in the study area. CaO and MgO content, which are representative of main components, range from 29.33% to 34.3%, with an average of 30.57% and 16.61% to 21.88%, with an average of 20.73%, respectively, and the Mg/Ca ratio is 0.48–0.73, with an average of 0.68. Na_2O and K_2O content which is representative of salinity is 0–0.11%, with an average of 0.03%.

For fine and medium crystalline dolomite in karst caves, SiO_2, TiO_2, and Al_2O_3 content is 0.01%, 0.0032%, and 0.03%, respectively. These are considerably lower than the contents of country rock dolomite, pointing out that they were from different diagenesis environments. TFe_2O_3 content is substantially higher (1.24%), and MnO content is lower (0.0157%). CaO content is 31.18% and MgO content is 20.54%, and the Mg/Ca ratio is 0.66. These characteristics are similar to those of the country rock

Table 1 Order degree of dolomite from the $Ma5^5$ and $Ma5^{10}$ sub-members of the Ordovician Majiagou Formationin the Jingxi area

Well	Depth (m)	Strata	Rock type	d(104)	I(015)	I(110)	Order degree
Z1	3881.7	$Ma5^5$	Micritic dolomite	2.88471	1045.23	1307.41	0.799
T18	3679.15	$Ma5^5$	Microcrystal dolomite	2.88515	925.82	1187.96	0.779
S373	4055.30	$Ma5^5$	Microcrystal dolomite	2.88661	724.27	969.29	0.747
T33	3119.65	$Ma5^5$	Microcrystal dolomite	2.88471	865.44	1218.83	0.710
L34	3960.40	$Ma5^5$	Power dolomite	2.88661	784.14	1021.39	0.768
S127	4118.08	$Ma5^5$	Power dolomite	2.88661	780.45	932.1	0.837
S22	3697.20	$Ma5^5$	Powder dolomite	2.88471	932.19	1083.5	0.860
T13	3625.93	$Ma5^5$	Power dolomite	2.888	793.46	1075.91	0.737
T38	3631.28	$Ma5^{10}$	Power dolomite	2.88515	1128.53	1288.1	0.876

Table 2 Element composition and $\delta^{13}C$, $\delta^{18}O$, and $^{87}Sr/^{86}Sr$ of dolomite from the $Ma5^5$–$Ma5^{10}$ sub-members of the Ordovician Majiagou Formationin theJingxi area

Well	Depth (m)	Strata	Rock type	Na_2O+K_2O (%)	SiO_2 (%)	TiO_2 (%)	Al_2O_3 (%)	TFe_2O_3 (%)	MnO (%)	MgO (%)	CaO (%)	Mg/Ca	$^{87}Sr/^{86}Sr$	$\delta^{13}C$ (‰)	$\delta^{18}O$ (‰)	Z(salinity index)
Z1	3880.68	$Ma5^5$	Micritic dolomite	0.1	1.59	0.0383	0.67	0.45	0.0404	21.24	29.33	0.72	0.709810	−0.676	−6.314	122.8
S198	3043.30	$Ma5^5$	Microcrystal dolomite	0	1.62	0.0174	0.26	0.22	0.0227	21.14	29.9	0.71	0.709892	−0.46	−6.659	123.0
Z5	3239.40	$Ma5^6$	Microcrystal dolomite	0.01	0.25	0.0048	0.05	0.32	0.0078	19.28	33.23	0.58	0.709664	−0.375	−8.493	122.3
T17	3780.30	$Ma5^{10}$	Microcrystal dolomite	0.04	0.52	0.0122	0.19	0.24	0.0292	21.63	29.8	0.73	0.709067	0.912	−5.423	126.5
T33	3112.14	$Ma5^5$	Power dolomite	0.01	0.75	0.0128	0.25	0.55	0.0218	21.45	30.17	0.71	0.710900	−0.564	−7.581	122.4
T18	3679.15	$Ma5^5$	Power dolomite	0.01	0.84	0.0082	0.18	0.19	0.0328	21.88	30.15	0.73	0.710487	0.301	−5.263	125.3
S203	3921.09	$Ma5^5$	Power dolomite	0.02	1.66	0.0221	0.49	0.27	0.0237	21.43	29.45	0.73	0.711807	−0.674	−6.267	122.8
S373	4055.30	$Ma5^5$	Power dolomite	0.01	1.78	0.014	0.18	0.23	0.0246	21.16	29.97	0.71	0.709110	−0.3	−6.055	123.7
S373	4059.13	$Ma5^5$	Power dolomite	0.01	1.64	0.0209	0.26	0.27	0.0291	19.65	31.72	0.62	0.709032	−1.446	−6.928	120.9
S379	3754.10	$Ma5^5$	Power dolomite	0.01	2.46	0.0111	0.17	0.2	0.025	20.99	29.79	0.70	0.709632	0.192	−5.783	124.8
L12	4107.10	$Ma5^5$	Power dolomite	0.01	2.4	0.0217	0.24	0.34	0.0275	20.99	29.45	0.71	0.709314	−0.42	−5.696	123.6
S127	4118.35	$Ma5^{10}$	Power dolomite	0.02	0.74	0.0084	0.21	0.3	0.0247	20.88	30.86	0.68	0.709302	−0.917	−6.732	122.1
S379	3798.02	$Ma5^6$	Power dolomite	0.11	2.91	0.0175	0.37	0.41	0.0225	16.61	34.3	0.48	0.709194	−2.137	−7.708	119.1
T38	3631.28	Ma5	Power dolomite	0.02	0.57	0.0083	0.18	0.18	0.0206	21.85	29.79	0.73	0.708922	−0.676	−6.396	122.7
S379	3812.02	$Ma5^6$	Karst cave fine and medium dolomite	0	0.01	0.0032	0.03	1.24	0.0157	20.54	31.18	0.66	0.709500	−1.497	−10.041	119.2

Note: Z=a ($\delta^{13}C$+50)+b($\delta^{18}O$+50), $\delta^{13}C$ and $\delta^{18}O$ are both PDB values，a=2.048, b=0.498 (from Keith and Weber, 1964).

dolomite. Na_2O and K_2O were not detected, indicating a lower salinity of diagenetic fluid than that of country rock dolomite.

4.3.2 Carbon, oxygen, and strontium isotopes

Results of carbon, oxygen, and strontium isotope tests are shown in Table 2. $\delta^{13}C$ values of country rock dolomite of $Ma5^5$–$Ma5^{10}$ sub-members in the study area range from −2.137‰ to 0.912‰, with an average of −0.517‰. $\delta^{18}O$ values range from −8.493‰ to 5.263‰, with an average of −6.521‰. Allan et al. (1993) proposed that $\delta^{13}C$ values of Ordovician seawater are between −2‰ and 0.5‰ and that $\delta^{18}O$ values are between −6.6‰ and −4.0‰. It is therefore known that the $\delta^{13}C$ values of country rock dolomite of the $Ma5^5$–$Ma5^{10}$ sub-members are similar to that of seawater in the same period, whereas $\delta^{18}O$ values of dolomite are significantly lower. The longitudinal change of $\delta^{18}O$ values shows that the correlation between $\delta^{18}O$ values and depths is not good as a whole, but for some local areas or a single well (such as Well S373 and Well S379), $\delta^{18}O$ values decrease as depth increases. On the plane, $\delta^{18}O$ values of dolomite from the $Ma5^5$ sub-member decrease from underwater uplifts in the sedimentary period (such as Well L12) to depressions (such as Well S203, Well S373, and Well S127).

$^{87}Sr/^{86}Sr$ values range from 0.7089 to 0.7118, with an average of 0.7097. Burke et al. (1982) proposed that the $^{87}Sr/^{86}Sr$ value of Ordovician seawater was about 0.7087, thus the $^{87}Sr/^{86}Sr$ values in the study area are significantly higher. By comparison, it is shown that there is a relationship between $^{87}Sr/^{86}Sr$ values and depth in the study area. Dolomites from the $Ma5^6$–$Ma5^{10}$ sub-members and deeper parts of the $Ma5^5$ sub-member are characterized by low $^{87}Sr/^{86}Sr$ values.

Fine and medium crystalline dolomite in karst caves have a $\delta^{13}C$ value of −1.497‰, a $\delta^{18}O$ value of −10.041‰, and a $^{87}Sr/^{86}Sr$ value of 0.7095. We therefore conclude that the $\delta^{13}C$ value of karst cave dolomite is similar to that of seawater in the same period. The $\delta^{18}O$ value is considerably lower than that of country rock dolomite and seawater in the same period. The $^{87}Sr/^{86}Sr$ value is similar to that of country rock dolomite in the same period.

4.4 Fluid inclusion of dolomite

Fluid inclusions of $Ma5^5$–$Ma5^{10}$ sub-members of the Ordovician Majiagou Formation in the study area mainly developed in powder dolomite near solution pores and solution pore–filling fine dolomite. Fluid inclusions are mainly in the following three occurrence states (Fig. 5): ① Isolated brine two-phase inclusions (WL+V); ② Brine two-phase inclusions (WL+V) and liquid brine inclusions (WL) distributed in cements of solution pores or fractures

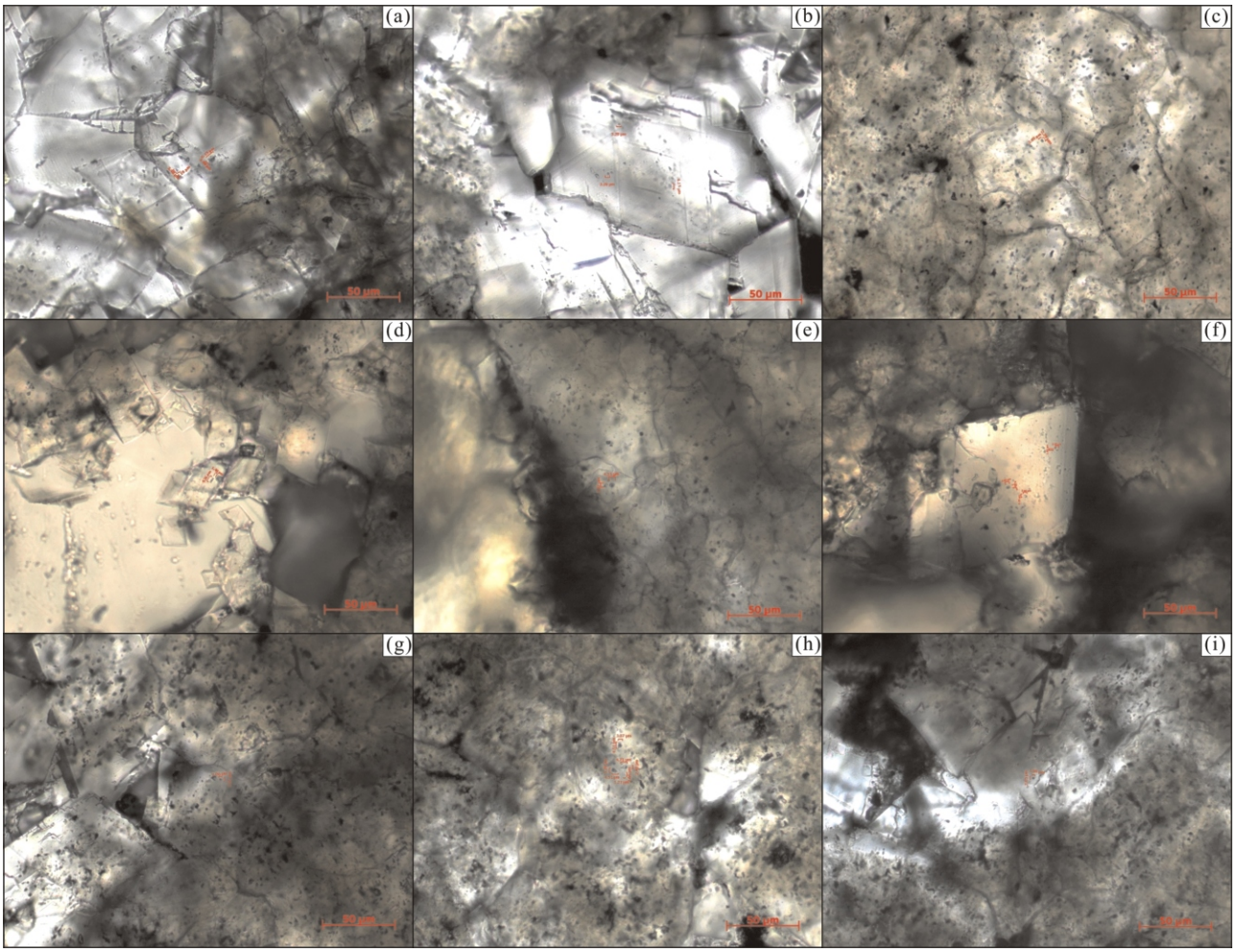

Fig. 5. Fluid inclusions in dolomite of the $Ma5^5$–$Ma5^{10}$ sub-members of the Ordovician Majiagou Formation in the Jingxi area.
(a), (b) Fine dolomite filled solution pores, WL,WL+V, and OV+WL distributed in groups (Well G039-22, $Ma5^5$, 3881.32 m); (c) Powder dolomite with fuzzy crystal boundary, recrystallization may have occurred, isolated WL+V (Well S373, $Ma5^5$, 4055.3 m); (d) Powder dolomite filled in solution pores, WL and WL+V distributed in groups (Well S345, $Ma5^5$, 3979.74 m); (e) Fine dolomite adjacent to solution pores, isolated WL+V (Well S345, $Ma5^6$, 4029.05 m); (f) Fine dolomite filled in solution pores, WL, WL+V, and OV+WL, distributed in groups (Well S345, $Ma5^6$, 4029.05 m); (g), (h) Powder dolomite adjacent to solution pores, isolated WL+V (Well S127, $Ma5^5$, 4119.59 m); (i) Powder dolomite filled in solution pores, isolated WL+V (Well S127, $Ma5^5$, 4119.59 m).

along two groups of perfect microfissures of dolomite, which are in the shape of moniliforms or groups; ③ Gaseous hydrocarbon-bearing brine inclusions (OV+WL) in cements of solution pores or fractures. The above-mentioned brine inclusions are generally small (2–5 μm).

In this study, we measured the homogenization and freezing temperatures of gas-liquid two-phase brine inclusions. We estimated the salinity according to the relation between salinity and freezing temperature (NaCleqv (wt% NaCl)= 0.000+1.78 Tm −0.042 Tm^2 +0.000557 Tm^3) (Hall et al., 1998). The results (Table 3) show that the homogenization temperature of inclusions in powder dolomite from country rock is 90.3°C–236.9°C, with an average of 136.59°C, and salinity is 6.88wt% NaCl–24.9wt%NaCl, with an average of 14.578wt%NaCl. The homogenization temperature of inclusions in powder dolomite and fine dolomite from cements of solution pores is 127.3°C–210.8°C, with an average of 173.16°C, and salinity is 17.61wt% NaCl–24.46wt% NaCl, with an average of 20.87wt%NaCl. As can be seen, both the homogenization temperature and salinity of inclusions in dolomite, both from country rock and cements of solution pores, vary greatly, which is related to complex secondary changes after the inclusions form.

5 Discussions

5.1 Microbial dolomite formed in syngenetic period

Primary dolomite can be deposited by anaerobic sulfate-reducing bacteria, methane-producing bacteria, and some aerobic bacteria under the participation of microorganisms (Vasconcelos, et al., 1995; Mazzullo, 2000; Chen Yongquan et al., 2008; McKenzie and Vasconcelos, 2009; You Xuelian et al., 2011; Mei Mingxiang, 2012). Spherical, dumbbell-shaped dolomite, especially nanometer nodular structure dolomite, has become the

Table 3 Gas-liquid brine inclusions in dolomite from the $Ma5^5$–$Ma5^{10}$ sub-members of the Ordovician Majiagou Formation in the Jingxi area

Well	Depth (m)	Interval	Host dolomite	Genetic type	Size (μm)	Homogeniz-ation temperature (°C)	Freezing point (°C)	Salinity (wt%NaCl)
G039-22	4007.72	$Ma5^5$	Fine dolomite filled in solution pore	Secondary	3.48×2.18	207.8	−23.2	24.46
G039-22	4007.72	$Ma5^5$	Fine dolomite filled in solution pore	Secondary	6.15×3.48	210.8	−19.4	21.96
G039-22	4007.72	$Ma5^5$	Fine dolomite filled in solution pore	Secondary	1.84×1.84	186.4	−18.7	21.47
G039-22	4007.72	$Ma5^5$	Fine dolomite filled in solution pore	Secondary	2.46×2.46	189.3	−17.9	20.89
G039-22	4007.72	$Ma5^5$	Fine dolomite filled in solution pore	Secondary	3.49×3.49	193.1	−17.7	20.75
G039-22	4007.72	$Ma5^5$	Fine dolomite filled in solution pore	Secondary	4.51×2.43	205.3	−18.1	21.04
S373	4055.3	$Ma5^5$	Power dolomite of country rock	Primary	2.05×2.79	129	4.7	7.45
S345	3979.74	$Ma5^5$	Fine dolomite filled in solution pore	Secondary	4.26×1.48	141.2	−15.2	18.8
S345	4029.05	$Ma5^6$	Power dolomite nearby solution pore	Secondary	4.31×2.87	236.9	−23.9	24.90
S345	4029.05	$Ma5^6$	Power dolomite nearby solution pore	Primary	3.48×2.87	120.5	−6.2	9.47
S345	4029.05	$Ma5^6$	Power dolomite nearby solution pore	Primary	1.64×1.64	170.8	−13.1	16.99
S345	4029.05	$Ma5^6$	Power dolomite nearby solution pore	Primary	3.89×3.28	179.5	−12.5	16.43
S345	4029.05	$Ma5^6$	Fine dolomite filled in solution pore	Secondary	2.25×1.02	158.7	−18	20.97
S345	4029.05	$Ma5^6$	Fine dolomite filled in solution pore	Secondary	2.93×2.09	162.1	−19.5	22.03
S345	4029.05	$Ma5^6$	Fine dolomite filled in solution pore	Secondary	2.66×2.25	171.3	−17.4	20.52
S127	4119.59	$Ma5^5$	Power dolomite of country rock	Primary	2.06×2.05	90.3	−4.3	6.88
S127	4119.59	$Ma5^5$	Power dolomite of country rock	Primary	4.1×2.22	100.7	−4.7	7.45
S127	4119.59	$Ma5^5$	Power dolomite of country rock	Primary	3.28×1.84	121.3	−17.8	20.82
S127	4119.59	$Ma5^5$	Power dolomite nearby solution pore	Primary	2.66×1.23	96.9	−17	20.22
S127	4119.59	$Ma5^5$	Power dolomite nearby solution pore	Primary	4.51×3.07	140.7	−11.3	15.27
S127	4119.59	$Ma5^5$	Power dolomite nearby solution pore	Primary	4.51×3.28	141.2	−11.5	15.47
S127	4119.59	$Ma5^5$	Power dolomite nearby solution pore	Primary	4.71×2.46	143.4	−11.2	15.17
S127	4119.59	$Ma5^5$	Power dolomite of country rock	Primary	1.84×1.64	121.3	−14.7	18.38
S203	3921.09	$Ma5^5$	Power dolomite nearby solution pore	Primary	4.3×3.69	119.8	−5.9	9.08
S127	4119.59	$Ma5^5$	Fine dolomite filled in solution pore	Secondary	2.25×1.43	207.3	−13.8	17.61
S127	4119.59	$Ma5^5$	Fine dolomite filled in solution pore	Secondary	3.28×2.87	132.6	−15.8	19.29
S127	4119.59	$Ma5^5$	Fine dolomite filled in solution pore	Secondary	4.2×2.76	127.3	−16.5	19.84
S127	4119.59	$Ma5^5$	Power dolomite filled in solution pore	Secondary	2.05×1.86	131.1	−20.3	22.58

main basis for identifying microbial dolomite (McKenzie and Vasconcelos, 2009; You Xuelian et al., 2011). Microscopic observations show that large amounts of clot dolomite and lamina dolomite occur in the study area. Sparry dolomites are mainly found among clots and laminae. Traces of algae bond occur in part particle dolomite. Based on the description of microbial mats by Mei Mingxiang (2014), it is possible that these dolomites are from microbial genesis to some extent. Horse tooth-like dolomite cements in part particle dolomite mainly formed in a shallow seawater environment, with high salinity around particles in the study area. These are very similar to horse tooth-like dolomite cements found in the Leikoupo Formation in the northwest region of the Sichuan Basin (Zeng Deming et al., 2006). SEM observations show spherical and short rod-like dolomite. Part-spherical dolomites are distributed in the form of moniliforms or chains, which are very similar to the previously proposed morphology of microbial dolomite (McKenzie and Vasconcelos, 2009; You Xuelian et al., 2011; Mei Mingxiang, 2012). The above dolomites were mainly distributed in the $Ma5^5$ and $Ma5^6$ sub-members of the Majiagou Formation in the Jingxi area, and are generally associated with gypsum rock, showing that they were formed in a high-salinity sedimentary environment. This is related to the occlusive epicontinental sea environment in the $Ma5^5$–$Ma5^{10}$ sub-members sedimentary period. The high sulfate content is conducive to the preservation of microbial activity and microbial dolomitization, thus the study area was fully equipped with conditions for formation of microbial dolomite in the $Ma5^5$–$Ma5^{10}$ sub-members sedimentary period. Clot, laminae, and other dolomites with algae bond in the study area may have experienced microbial dolomitization. Dolomites formed in this stage are mostly micritic dolomite and horse tooth-like dolomite cements, which developed in a relatively low-energy subtidal-intertidal zone. This is consistent with the shallow sea-supratidal zone environment favorable to dolomite distribution proposed by Huang Sijing (2010).

5.2 Seepage reflux dolomite in the penecontemporaneous period and the secondary change of dolomite in the burial stage

5.2.1 Element composition

According to the relationship of CaO and MgO contents in the study area (Fig. 6), we judged that there is a weak positive correlation when CaO content is low and a negative correlation, to some extent, when CaO content is high. This marks the diversity of genetic types of dolomite in the study area. However, the CaO content of most samples is low and concentrated, indicating the dolomite

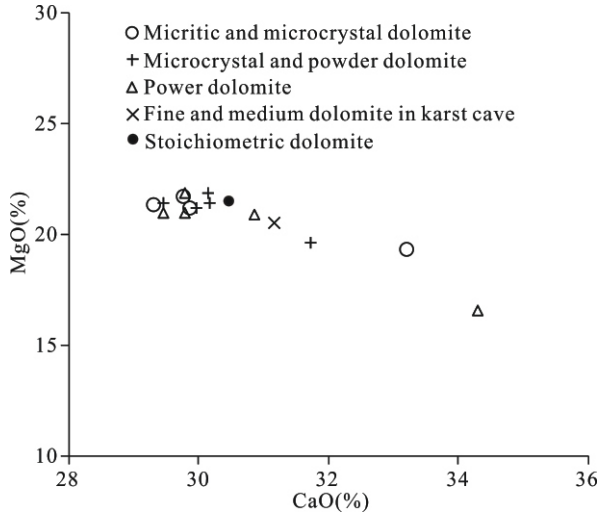

Fig. 6. Dolomite composition and distribution of CaO and MgO content in the $Ma5^5$–$Ma5^{10}$ sub-members of the Ordovician Majiagou Formation in the Jingxi area.

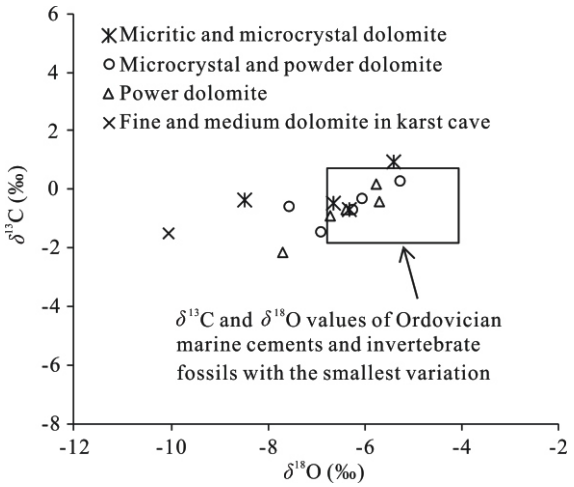

Fig. 7. Distributions of $\delta^{13}C$ and $\delta^{18}O$ of dolomite in $Ma5^5$–$Ma5^{10}$ sub-members of the Ordovician Majiagou Formation in Jingxi area.

should be mainly from metasomatic genesis. The CaO and MgO contents of dolomite vary greatly in the study area, whereas the compositions of most dolomites are close to stoichiometric dolomite (30.4% CaO and 21.7% MgO), implying that the metasomatic degree of most dolomite is relatively high. In addition, compared with karst cave dolomite, country rock dolomite is high in SiO_2, TiO_2, Al_2O_3, and Na_2O+K_2O, and low in TFe_2O_3, signaling the genesis of high-salinity near-surface seawater.

5.2.2 Carbon and oxygen isotopes

$\delta^{13}C$ and $\delta^{18}O$ are commonly employed to trace the generation and epigenesis of carbonate particles. Preservation of $\delta^{13}C$ and $\delta^{18}O$ depends on the extent of preservation of primary mineral and diagenetic alteration. Therefore, genesis of $\delta^{13}C$ and $\delta^{18}O$ of dolomite needs to be compared with that of seawater in the geological history. Stable carbon and oxygen isotope values of seawater in the geological history cannot generally be measured directly, but they can be estimated by measuring stable isotope values of marine cements and invertebrate fossils with the smallest variation. Allan (1993) counted the range of variation of stable carbon and oxygen isotope values of marine cements and invertebrate fossils with the smallest variation made by different scholars. The $\delta^{18}O$ of the maximum amplitude of variation was taken as the value with minimum variation. The most positive $\delta^{18}O$ in the maximum amplitude of variation and the most positive $\delta^{18}O$ in the minimum amplitude of variation were taken as the upper and lower limits of the baseline of seawater in every geological period. In this way, the distribution of seawater $\delta^{18}O$ in the period can be more reasonably reflected. Distribution of seawater $\delta^{13}C$ in the geological periods can be obtained using similar methods. Therefore, stable carbon and oxygen isotope values of Ordovician seawater are about −2.0‰–0.5‰ and −6.6‰–−4.0‰, respectively. The $\delta^{13}C$ of country rock dolomite in the $Ma5^5$–$Ma5^{10}$ sub-members of the Ordovician Majiagou Formation in the study area is close to that of the seawater from the same period. $\delta^{18}O$ is partly in the scope of seawater, but it is still relatively negative as a whole and similar to that of the average value of seawater. The maximum negative value is only 3.193‰ (Fig. 7).

$\delta^{18}O$ negative distribution of dolomite is often caused by the influence of temperature or meteoric fresh water. It was dry and hot during the sedimentary period of the Ma5 member of the Ordovician Majiagou Formation in the study area. There was little meteoric fresh water in the penecontemporaneous period, but a lot of meteoric fresh water may have infiltrated into carbonate rocks during the supergene period of the late Ordovician, which may have had some impacts on carbonate rocks during the burial process. Temperature plays an important role in oxygen isotope fractionation in carbonate minerals. Dolomites formed at higher temperatures are generally characterized by a greatly negative $\delta^{18}O$, with a magnitude that is often more than 4‰–5‰, which obviously exceeds the maximum negative value in the area. Except for the fine and medium crystalline karst cave dolomite showing the obvious negative $\delta^{18}O$ to indicate that the dolomite is formed at high temperatures in deep burial process, the study area concentrates on powder, microcrystal, and micritic structure with few examples of medium and coarse crystalline dolomite. It also indicates that the metasomatism at high temperatures should not be the main cause of significantly negative $\delta^{18}O$ values in country rock dolomite.

In fact, dolomite generally occurs in a quasi-stable phase at birth (Land, 1980, 1985) and is prone to recrystallization. Also, isotope reequilibration can occur during the burial process (Wang Xiaolin et al., 2010; Hu Mingyi et al., 2011; Zhu Dongya et al., 2012). Complex mineral characteristics in dolomite also affect dolomite's final stability and isotopic composition (Reeder, 1981, 1983). Therefore, in many cases, dolomite isotopic composition is more likely to indicate the nature of the recrystallization fluid than the components of the diagenetic fluid of primary dolomitization (Moore, 2001). Dolomite recrystallization and stabilization results in low $\delta^{18}O$, which may lead to the loss of oxygen isotopic characteristics at low temperatures for dolomite formed in a seawater environment during the burial process. The oxygen isotopic characteristics of dolomite in the study area are possibly the result of recrystallization or neomorphism of dolomite formed in a seawater environment during the burial process. Cathodoluminescence characteristics of dolomite also provide corresponding evidence. Dolomites in the study area mostly emit dim light under cathodoluminescence, and parts of dolomite edges emit bright light, announcing the dolomites should be the genesis of seawater, and dolomite edges emitting bright light may be caused by adjustment of diagenetic fluid in the burial stage. Dolomite is characterized by high order degree and high fluid inclusion homogenization temperatures with a large range of variations that may also be the results of adjustment of dolomite in the burial process.

Dolomite formed under seawater conditions is possibly seawater seepage reflux dolomite, except for the previously mentioned microbial dolomite. Evaporation in the $Ma5^4$ sub-member is stronger than in the $Ma5^5$ sub-member, thus the anhydrite layer that developed in the $Ma5^4$ sub-member is in line with the general pattern of seepage reflux dolomitization. The dolomite salinity index (Z), which is calculated using $\delta^{13}C$ and $\delta^{18}O$ (Keith and Weber, 1964), is generally more than 120, specifying genesis from evaporation of seawater. $\delta^{18}O$ becomes lower from underwater uplifts (such as the uplift in the area on the western edge and the local uplift of the Jingbian-Wuqi belt) to depressions and from shallow parts to deep parts. Dolomite types along this direction change from fine dolomite to micritic and micro dolomite and dolomite content decreases. Therefore, the main migration direction of dolomitizing fluid is from shallow parts to deep parts and from underwater uplifts to depressions, showing the characteristics of seepage reflux.

5.2.3 Strontium isotope

$^{87}Sr/^{86}Sr$ in seawater is mainly affected by continental crust and oceanic crust. Continental crust has a higher $^{87}Sr/^{86}Sr$ than oceanic crust, and can be transported to seawater by continental weathering and marine hydrothermal processes. Therefore, $^{87}Sr/^{86}Sr$ in seawater

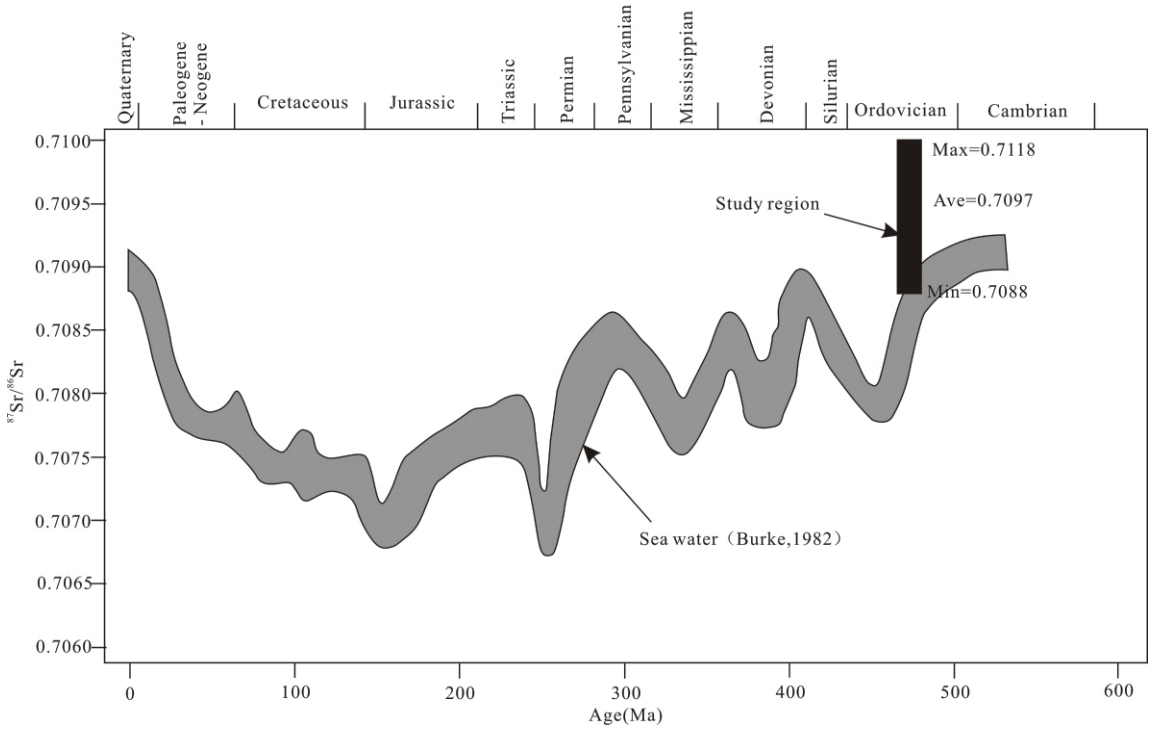

Fig. 8. Distribution of $^{87}Sr/^{86}Sr$ of dolomite in the $Ma5^5$–$Ma5^{10}$ sub-members of the Ordovician Majiagou Formation in the Jingxi area.

changes over time due to the impact of global tectonic movements (Burke et al., 1982; Huang et al., 2016). The $^{87}Sr/^{86}Sr$ of country rock dolomite in the study area is similar to that of karst cave filling dolomite and substantially higher than that of Ordovician seawater (Fig. 8).

The study area was a relatively occlusive epicontinental sea environment during the Majiagou Formation sedimentary period and faults were not developed. Therefore, the impact of marine hydrothermal solution or deep hot water can be neglected. Uplift and erosion during the late Caledonian resulted in the Central Ancient Uplift being influenced by meteoric fresh water for a long time, which would carry $^{87}Sr/^{86}Sr$ from siliciclastic material into diagenetic fluids. Karst cave filling dolomite may have been formed by $^{87}Sr/^{86}Sr$-rich mixing fluid during the late burial stage. However, these are not directly dolomitizing fluids for country rock dolomite because they were formed after the Caledonian uplift and erosion period whereas the dolomite had already been formed by microbial and seepage reflux dolomitization. Due to strong adjustment and reform by burial closed fluid in late stage, country rock dolomite is characterized by high $^{87}Sr/^{86}Sr$, which overshadowed the $^{87}Sr/^{86}Sr$ of fluid when dolomite was formed. There is a negative correlation between the $^{87}Sr/^{86}Sr$ of country rock dolomite and burial depth, namely that the $^{87}Sr/^{86}Sr$ of the $Ma5^6$–$Ma5^{10}$ sub-members and part of the $Ma5^5$ sub-member with a greater burial depth is lower than that of relatively shallow parts of the $Ma5^5$ sub-member. This indicates that the above mixed diagenetic fluid is related to weathering and erosion and shows that country rock dolomite was affected by mixed fluid in a late stage rather than being formed directly by burial dolomitization because deep burial closed fluid is always characterized by high $^{87}Sr/^{86}Sr$ (such as dolomite formed in karst caves in the $Ma5^6$ sub-member).

5.2.4 Fluid inclusion

Fluid inclusion preserves the original record of diagenetic fluid, but its internal pressure and temperature conditions will change accordingly when it is buried and heated, or when deformation or a leak occurs, causing variations in measured temperature (*T*h) and salinity (*T*m) (Burruss, 1987; Allan, 1993; Goldstein, 2001; Ayllon et al., 2003). A Th-Tm crossplot can provide valuable information on how inclusions evolved after being trapped (Roedder, 1981; Parnell, 2010; Terrence, 2015). As can be seen in Fig. 9, primary inclusions of dolomite around solution pores show dispersion characteristics of subpopulations, suggesting that they have experienced rupture and reequilibration. A Th-Tm crossplot of secondary inclusions of solution-pore filling dolomite-

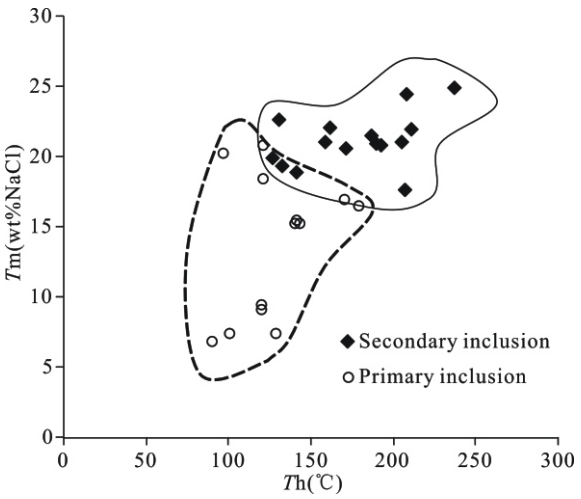

Fig. 9. Temperature-Salinity (Th-Tm) crossplot of fluid inclusions in dolomite in the $Ma5^5$–$Ma5^{10}$ sub-members of the Ordovician Majiagou Formation in the Jingxi area.

shows a positive correlation to some extent, implying evolution of the coexistence of deformation and rupture. Therefore, the homogenization temperature and salinity of fluid inclusions in dolomite in the study area cannot really reflect original fluid properties, but can determine the upper limit of dolomite formation temperature and identify the late stage adjustment of burial fluid.

It is known from test data results that when country rock dolomite was formed, fluid temperature and salinity were likely to be lower than 90.3°C and 6.88wt%NaCl, respectively. When solution-pore filling dolomite-was formed, fluid temperature and salinity was possibly lower than 127.3°C and 17.61wt%NaCl, respectively. Therefore, we can conclude that both country rock dolomite and solution-pore filling dolomite experienced strong burial adjustment effects.

5.3 Dolomitization pattern

Based on the above analysis and taking $Ma5^5$ sub-member dolomite as an example, we can establish the dolomitization pattern in the study area (Fig. 10). During the syngenetic stage, the $Ma5^5$ sub-member in the study area experienced dolomitization related to microorganisms in the development position of lamellar sediments, sand debris sediments, mud, and other fine-grained sediments, and mainly formed micrite dolomite to provide good fluid migration pathways for the following seepage reflux dolomitization. In the penecontemporaneous stage, evaporation seawater with increased Mg/Ca refluxed to deep parts and depressions due to increased density influenced by a hypersaline water depositional environment and evaporite sediments during the $Ma5^4$ period, resulting in wide dolomitization in the $Ma5^5$ sub-

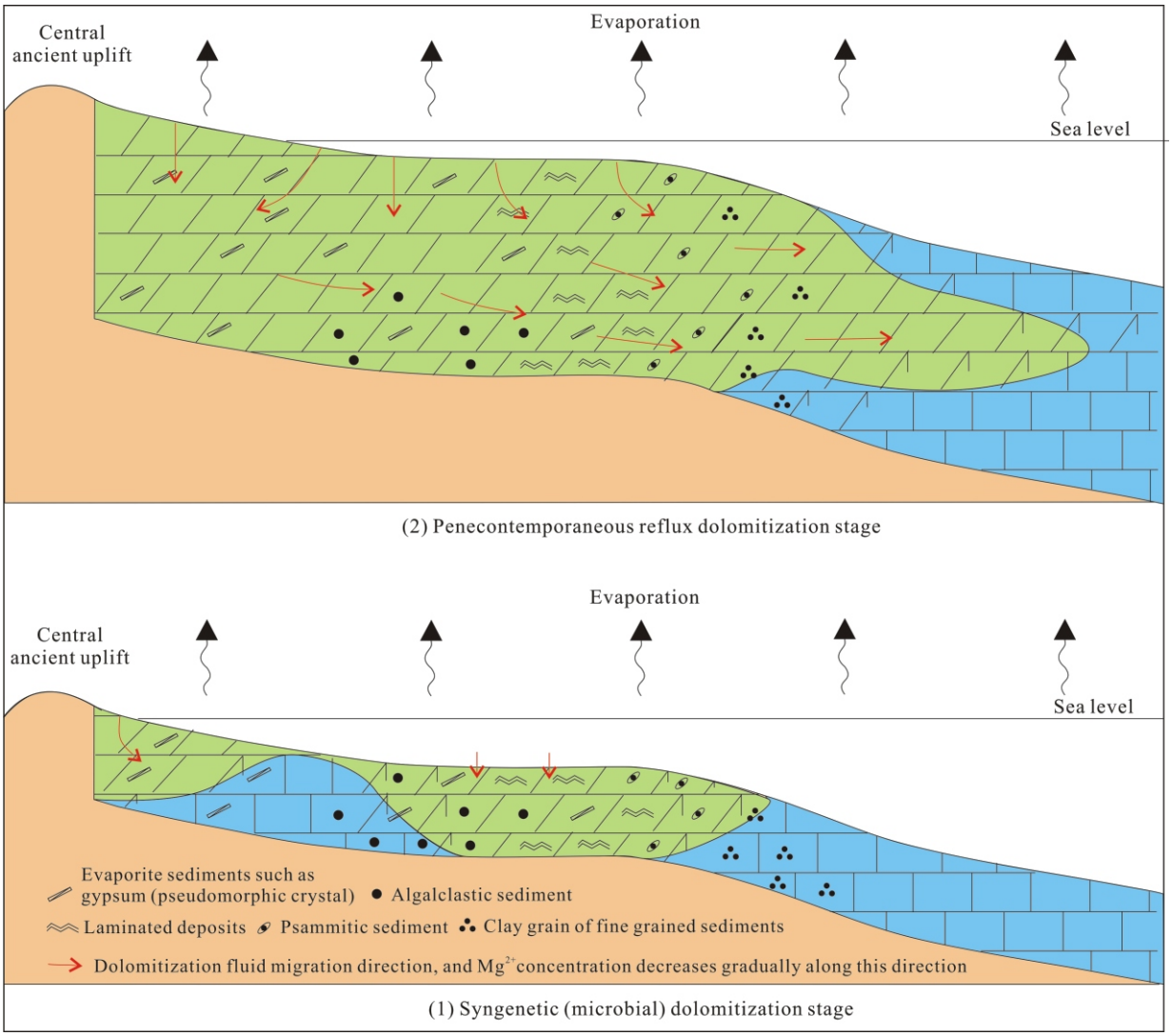

Fig. 10. Dolomitization patterns in the $Ma5^5$ sub-member in the Jingxi area.

member. Mg^{2+} concentration decreased gradually in the direction of dolomitization fluid migration and the degree of dolomitization decreased constantly. Seepage reflux dolomitization is the most important formation mechanism of dolomite in the study area. In the middle-deep burial stage, the formation contained a mix of closed epidiagenetic meteoric fresh water and residual evaporation. This fluid resulted in obvious recrystallization, stabilization, and other important adjustments to the formed dolomite. At the same time, burial fluid formed euhedral dolomite cements in partial solution pores and fractures. The sedimentary and burial history of the $Ma5^7$–$Ma5^6$ and $Ma5^9$–$Ma5^8$ sub-members is similar to that of the $Ma5^5$–$Ma5^4$ sub-members. The dolomitization mechanism is the same. A significant regression evaporation environment developed in the $Ma5^6$ and $Ma5^8$ sub-members, especially in the $Ma5^6$ sub-member. This environment can provide a great deal of Mg^{2+}, creating favorable conditions for wide seepage reflux dolomitization in the $Ma5^7$ and $Ma5^9$ sub-members and forming large-scale dolomite.

5.4 The impact of dolomitization in each period on reservoir properties

Different genetic types of dolomite have different effects on the porosity of rock. Dolomite formed by microbial dolomitization is no more porous than limestone, but its strong ability to resist compaction means that more original pores are preserved and that it is conducive to dolomitization fluid flow, promoting seepage reflux dolomitization. Seepage reflux dolomitization, which is the main source of dolomitization in study area, is dominantly of metasomatic origin. Due to the high specific gravity and small volume, metasomatizing the same amount of calcite will increase the total porosity of rock by approximately 13% (Moore, 2001). But porosity

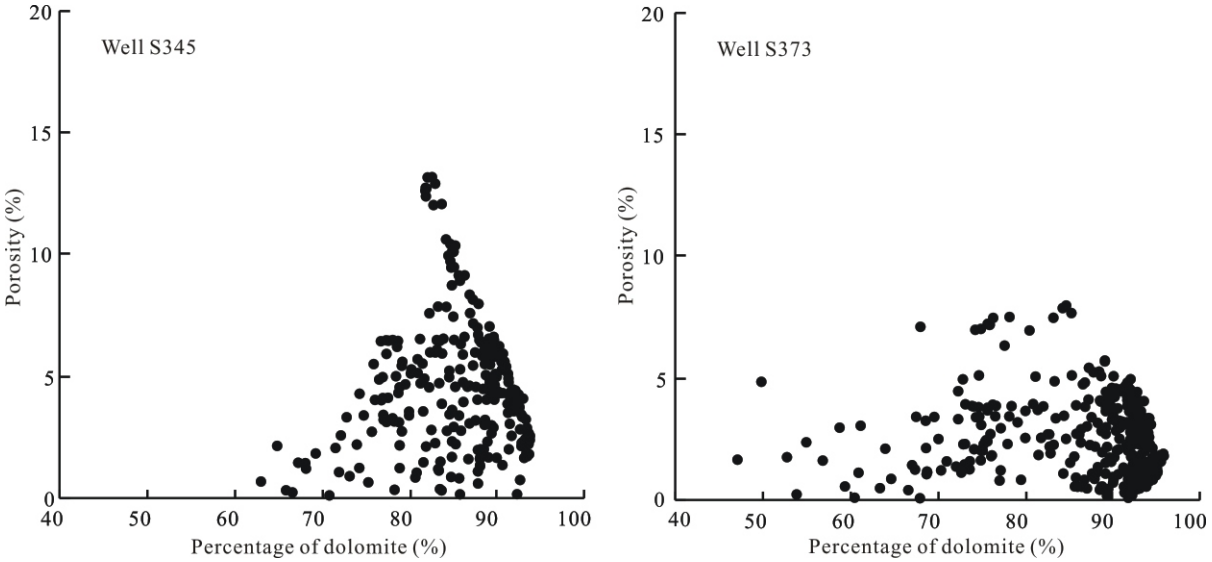

Fig. 11. Relationship between porosity and percentage of dolomite in the $Ma5^5$–$Ma5^{10}$ sub-members of the Ordovician Majiagou Formation in the Jingxi area.

increases caused by dolomitization are not absolute, and sometimes dolomitization may decrease porosity, which is associated with dolomite content.

The $Ma5^5$–$Ma5^{10}$ sub-members mainly experienced dolomitization during the penecontemporaneous stage, and then experienced epigenic karstification and buried karstification. Intercrystalline calcites are often dissolved, so it is not the case that a higher dolomitization degree means better porosity. Statistical results showed that, to some extent, the porosity of the $Ma5^5$–$Ma5^{10}$ sub-members was controlled by dolomite content. Porosity increases with dolomite content when dolomite content is below about 85% and decreases when dolomite content is more than about 85% (Fig. 11). Permeability also increases with dolomite content. Dolostone with higher dolomite content is more likely to form fractures during burial or tectonic processes, which can effectively increase the permeability of rock, so when dolomite content is higher, porosity may be lower, but permeability still exhibits a higher value. Buried karstification mainly formed dolomite overgrowths and pore- and fracture-filling dolomite cement. This dolomitization plays a role in filling the reservoir in study area. Although the distribution of this dolomitization is wide, its development is relatively low and the damage to reservoir pores is limited.

5.5 The spatial distribution of dolomitization in each stage and the prediction of favorable exploration areas

According to the above analysis, the formation of dolostone of the $Ma5^5$–$Ma5^{10}$ sub-members experienced microbial dolomitization during the contemporaneous stage, seepage reflux dolomitization during the penecontemporaneous stage, and buried dolomitization during the middle and deep buried stage. Although microbial dolomitization in the contemporaneous stage is not the main dolomitization, it mainly developed in the intertidal to subtidal zones where fine sediments developed in the eastern portion of study area. Buried dolomitization was widely distributed during buried processes, but the development degree is limited. Diagenetic fluid sealed earlier and associated with meteoric freshwater during the epigenetic stage evolved into dolomitization fluid at higher temperatures and reformed the early dolostone or took the form of dolomite cement. This kind of dolomitization is mainly distributed in the range reflected by meteoric freshwater in the epigenetic stage. Seepage reflux dolomitization during the penecontemporaneous stage is the most important dolomitization forming dolostone and is the main cause of the distribution of dolostone currently. Along the migration direction of dolomitization fluid, the dolomitization degree and dolomite content gradually decrease and the crystalline grain becomes fine. So, the favorable position of dolostone is underwater uplift and slope in the penecontemporaneous stage, which is conducive to the formation of intergranular pores. The analysis of the sedimentary environments of the $Ma5^5$–$Ma5^{10}$ sub-members in the study area shows that the Wuqi-Jingbian-Hengshan areas were the underwater uplift and slope at that time, which was the most conducive to forming dolostone and is a favorable area for further oil and gas exploration.

6 Conclusions

(1) We clarified three main stages of dolomitization and

secondary change by studying the petrology and geochemistry characteristics of dolomite from the $Ma5^5$–$Ma5^{10}$ sub-members of the Ordovician Majiagou Formation in the Jingxi area in the Ordos Basin: ① Syngenetic microbial dolomitization is characterized by formation of dolomite with a mainly micrite structure and horse tooth-shape dolomite cements. ② Seepage reflux dolomitization during the penecontemporaneous period superposed adjustment functions such as recrystallization and stabilization in the middle-deep burial stage, and formed mainly microcrystalline and powder dolomite. ③ Powder-fine and medium-coarse crystalline dolomite formed in pores and fractures in the middle-deep burial stage.

(2) The occurrence of many stages of dolomitization is mainly controlled by the secondary concussive transgression-regression under a regressive background. A high salinity sedimentary environment and high sulfate content are conducive to the preservation of microbial activity and precipitation of primary dolomite. Affected by evaporation seawater with increased Mg/Ca ratio in the $Ma5^4$, $Ma5^6$, and $Ma5^8$ sub-members, seepage reflux dolomitization was widely developed and large-scale dolomite was formed. Mixed fluid composed of closed epidiagenetic meteoric fresh water and residual evaporation seawater in the middle-deep burial stage formed a small amount of euhedral dolomite in pores and fractures at high temperatures and also resulted in recrystallization or stabilization to form dolomite.

(3) The porosity increases with increasing dolomite content when the dolomite content is below about 85%, but decreases when dolomite content is more than about 85%. Permeability increases with increasing dolomite content. Affected by seepage reflux dolomitization, many intergranular pores were formed, and underwater uplifts and slope at that time are favorable areas of dolostone distribution.

Acknowledgments

This work is granted by the Fundamental Research Funds for the Central Universities (14CX02116A) and the Foundation of State Key Laboratory of Petroleum Resources and Prospecting, China University of Petroleum, Beijing (No. PRP/open-1604).

Manuscript received May. 6, 2016
accepted Jan. 12, 2017
edited by Liu Lian

References

Allan, J.R., and Wiggins, W.D., 1993. Dolomite reservoirs: Geochemical techniques for evaluating origin and distribution. *AAPG Continuing Education Course Notes Series No. 36.* Tulsa: AAPG, 36–129.

Ayllon, F., Bakker, R.J., and Warr, L.N., 2003. Re-equilibration of fluid inclusions in diagenetic-anchizonal rocks of the Cinera–Matallana coal basin (NW Spain). *Geofluids,* 3(1): 49–68.

Bi, Shengyu, Zheng, Congbin, Li Zhenhong and Ma Junbao, 2005. Origin of Dolomite Mass of Tianhuan Northern Section in Ordos Basin. *Journal of East China Institute of Technology*, 28(1): 1–4 (in Chinese with English abstract).

Burke, W.H., Denison, R.E., Hetherington, E.A., Koepnick, R.B. Nelson, H.F., and Otto, J.B., 1982. Variation of seawater $^{87}Sr/^{86}Sr$ throughout Phanerozoic time. *Geology*, 10: 516–519.

Burruss, R.C., 1987. Diagenetic paleotemperatures from aqueous fluid inclusions re-equilibration of inclusions in carbonate cements by burial heating. *Mineral Mag*, 51: 477–481.

Chen Hongde, Hu Sihan, Chen Anqing, Zhao Junxing and Su Zhongtang, 2013. Genesis of non-karst dolomite reservoirs in the eastern central paleo-uplift in the Ordos Basin. *Natural Gas Industry*, 33(10): 18–24 (in Chinese with English abstract).

Chen Yongquan, Zhou Xinyuan, Zhao Kuidong, Yang Wenjing, Dong Chenyang and Zhu Changjian, 2008. Geochemical research on straticulate dolostone and spatulate dolostone in lower Ordovician strata of Well Tazhong-1, Tarim Basin. *Acta Geologica Sinica*, 82(6): 826–834 (in Chinese with English abstract).

Fu Jinhua, Wang Baoqing, Sun Liuyi, Bao Hongping and Xu Bo, 2011. Dolomitization of Ordovician Majiagou Formation in Sulige region, Ordos Basin. *Petroleum Geology and Experiment*, 33(3): 266–273 (in Chinese with English abstract).

Goldstein, R.H., 2001. Fluid inclusions in sedimentary and diagenetic systems. *Lithos*, 55: 159–193.

Hall, D.L., Sterner, S.M., and Bondnar, R.J., 1998. Freezing point depression of NaCl-KCl-H_2O solutions. *Economic Geology*, 83: 197–202.

He, X.Y., Shou, J.F., Shen, A.J., Wu, X.G., Wang, Y.S., Hu, Y.Y., Zhu, Y., and Wei, D.X., 2014. Geochemical characteristics and origin of dolomite: A case study from the middle assemblage of Majiagou Formation Member 5 of the west of Jingbian Gas Field, Ordos Basin, North China. *Petroleum Exploration and Development*, 41(3): 375–384.

Hou Fanghao, Fang Shaoxian, Dong Zhaoxing, Li Ling, Lu Shuxiu, Wu Yi and Chen, Yana, 2003. Developmental characters of sedimentary environments and lithofacies of Middle Ordovician Majiagou Formation in Ordos Basin. *Acta Sedimentologica Sinica*, 21(1): 106–112 (in Chinese with English abstract).

Hu Mingyi, Hu Zhonggui, Li Sitian and Wang Yanqi, 2011. Geochemical characteristics and genetic mechanism of the Ordovician dolomite in Tazhong area, the Tarim Basin. *Acta Geologica Sinica*, 85(12): 2060–2069 (in Chinese with English abstract).

Huang, K.K., Zhong, Y.J., Huang, S.J., LI, X.N., and Feng, M.S., 2016. Saddle-Dolomite-Bearing Fracture Fillings and Records of Hot Brine Activity in the Jialingjiang Formation, Libixia Section, Hechuan Area of Chongqing City. *Acta Geologica Sinica* (English Edition), 90(1): 195–208.

Huang Qingyu, Zhang Shaonan, Ding Xiaoqi, Duan Jie and

Xiang Lei, 2010. Origin of dolomite of Ordovician Majiagou Formation, western and southern margin of the Ordos Basin. *Petroleum Geology and Experiment*, 32(2): 147–153 (in Chinese with English abstract).

Huang Sijing, 2010. *Carbonate diagenesis.* Beijing: Geological Publishing House (in Chinese).

Huang Zhengliang, Bao Hongping, Ren Junfeng, Bai Haifeng and Wu Chunying, 2011. Characteristics and genesis of dolomite in Majiagou Formation of Ordovician, south of Ordos Basin. *Geoscience*, 25(5): 925–930 (in Chinese with English abstract).

Huang Zhengliang, Chen Tiaosheng, Ren Junfeng and Bao Hongping, 2012. The characteristics of dolomite reservoir and trap accumulation in the middle assemblages of Ordovician in Ordos Basin, China. *Acta Petrolei Sinica*, S2: 118–124 (in Chinese with English abstract).

Huang Zhengliang, Liu Yan, Wu Chunying, Wang Qianping and Ren Junfeng, 2014. Characteristics of hydrocarbon accumulation in the middle and lower sections of middle assemblages of lower Ordovician Majiagou Member-5, Ordos Basin. *Marine Origin Petroleum Geology*, 19(3): 57–65 (in Chinese with English abstract).

Keith, M.L., and Weber, Y.N., 1964. Carbon and oxygen isotopic composition of selected limestone and fossils. *Geochimica et Cosmochimica Acta*, 28: 1787–1816.

Land, L.S., 1980. The isotopic and trace element geochemistry of dolomite: The state of the art. *SEPM Special Publication*, 28: 87–110.

Land, L.S., 1985. The origin of massive dolomite. *Journal of Geological Education*, 33: 112–125.

Mazzullo, S.J., 2000. Organogenic dolomitization in peritidal to deep sea sediments. *Journal of Sedimentary Research*, 70(1): 10–23.

McKenzie, J.A., and Vasconcelos, C., 2009. Dolomite mountains and the origin of the dolomite rock of which they mainly consist: Historical developments and new perspectives. *Sedimentology*, 56: 205–219.

Mei, Mingxiang, 2012. Brief introduction of "dolostone problem" in sedimentology according to three scientific ideas. *Journal of Palaeogeography*, 14(1): 1–12 (in Chinese with English abstract).

Mei Mingxiang, 2014. Feature and nature of microbial-mat: Theoretical basis of microbial-mat sedimentology. *Journal of Palaeogeography*, 16(3): 285–304 (in Chinese with English abstract).

Moore, C.H., 2001. *Carbonate reservoirs: porosity evolution and diagenesis in a sequence stratigraphic framework.* Translated by Yao Genshun, Shen Anjiang, Pan Wenqing, Zheng Jianfeng, Luo Xianying and Han Jianfa, Beijing: Petroleum Industry Press, 55 (in Chinese).

Parnell, J., 2010. Potential of paleofluid analysis for understanding oil charge history. *Geofluids*, 10: 73–82.

Reeder, R.J., 1981. Electron optical investigation of sedimentary dolomites. *Contributions to Mineralogy and Petrology*, 76:148–157.

Reeder, R.J., 1983. Crystal chemistry of the rhombohedral carbonates. *Reviews in Mineralogy and Geochemistry*, 11: 1–47.

Roedder, E., 1981. Origin of fluid inclusions and changes that occur after trapping. In Hollister L.S., Crawford M.L., eds., short course in fluid inclusions: application to petrology. *Mineralogical Assoc Canada*, 6: 101–137.

Shi Baohong, Liu Yanan, Wu Chunying, Huang Zhenliang and Ren Junfeng, 2013. Geological conditions for hydrocarbon accumulation in middle reservoir-source rock combination of the Ordovician Majiagou Formation on the east side of the paleo-uplift in Ordos Basin. *Oil &Gas Geology*, 34(5): 610–618 (in Chinese with English abstract).

Su Zhongtang, Chen Hongde, Xu Fenyan and Jin Xueqiang, 2013. Genesis and reservoir property of lower Ordovician Majiagou dolostones in Ordos Basin. *Marine Origin Petroleum Geology*, 18(2): 15–22 (in Chinese with English abstract).

Su Zhongtang, Chen Hongde, Xu Fenyan, Wei Liubin and Li Jie, 2011. Geochemistry and dolomitization mechanism of Majiagou dolomites in Ordovician, Ordos, China. *Acta Petrologica Sinica*, 27(8): 2230–2238 (in Chinese with English abstract).

Su Zhongtang Chen Hongde, Zhao Junxing, Hou Mingcai and Hao Yi, 2008. The diagenesis character in Member 5–4–1 of Ordovician Majiagou Formation and its petroleum geology significance in the north of Jingbian gasfield, Ordos basin, China. *Journal of Chengdu University of Technology* (Science & Technology Edition), 35(2): 194–200 (in Chinese with English abstract).

Terrence, P.M., 2015. A Review of fluid inclusions in diagenetic systems. *Acta Geologica Sinica* (English Edition), 89(3): 697–714.

Vasconcelos, C., McKenzie, J.A., and Bernasconi, S., 1995. Microbial mediation as a possible mechanism for natural dolomite formation at low temperatures. *Nature*, 377: 220–222.

Wang Baoquan, Qiang Zitong, Zhang Fan, Wang Xingzhi, Wang Yi and Cao Wei, 2009. Isotope characteristics of dolomite from the fifth member of the Ordovician Majiagou Formation, the Ordos Basin. *Geochimica*, 38(5): 472–479 (in Chinese with English abstract).

Wang Xiaolin, Hu Wenxuan, Chen Qi, Li Qing, Zhu Jingquan and Zhang Juntao, 2010. Characteristics and formation mechanism of Upper Sinian algal dolomite at Kalpin area, Tarim Basin, NW China. *Acta Geologica Sinica*, 84(10): 1479–1494 (in Chinese with English abstract).

Yang Hua and Bao Hongping, 2011. Characteristics of hydrocarbon accumulation in the middle Ordovician assemblages and their significance for gas exploration in the Ordos Basin. *Natural Gas Industry*, 31(12): 11–20 (in Chinese with English abstract).

Yang Hua, Liu Xinshe and Zhang Daofeng, 2013. Main controlling factors of gas pooling in Ordovician marine carbonate reservoirs in the Ordos Basin and advances in gas exploration. *Natural Gas Industry*, 33(5): 1–12 (in Chinese with English abstract).

Yang Hua, Wang Baoqing, Sun Liuyi, Ren Junfeng, Huang Zhengliang and Wu Cunying, 2012. Characteristics of oxygen and carbon stable isotopes for middle Ordovician Majiagou Formation carbonate rocks in the Ordos basin. *Natural Gas Geoscience*, 23(4): 616–625 (in Chinese with English abstract).

Yao, J.L., Wang, B.Q., Wang, Y., Huang, D.J., and Wen, C.X., 2009. Geochemical characteristics of dolomites in Lower Ordovician Majiagou Formation, Ordos Basin. 2011, *Acta Sedimentologica Sinica*, 27(3): 381–389.

You, X.L., Sun, S., Zhu, J.Q., Liu, L., and He, K., 2011. Progress in the study of microbial dolomite model. *Earth Science Frontiers*, 18(4): 052–064.

Yu Zhou, Sun Liuyi, Wu Xingning, Wu Dongxu, Yao Xuehui and Ding Zhenchun, 2012. Characteristics and controlling factors of the Middle Array of Ordovician Majiagou reservoirs to the west of Jingbian Gas Field, Ordos Basin. *Marine Origin Petroleum Geology*, 17(4): 49–56 (in Chinese with English abstract).

Zeng Deming, Wang Xingzhi and Kang Baoping, 2006. A study on cement in primary pore of the leikoupo formation reservoir in the Northwest of Sichuan Basin. *Natural Gas Geoscience*, 17(4): 459–462 (in Chinese with English abstract).

Zhang Yongsheng, 2000. Mechanism of deep burial dolomitization of massive dolostones in the Middle Majiagou Group of the Ordovician, Ordos Basin. *Acta Sedimentologica Sinica*, 18(3): 424–430 (in Chinese with English abstract).

Zhao Junxing, Chen Hongde, Zhang Jinquan, Liu Xiaoli and Fu Suotang, 2005. Genesis of dolomite in the fifth member of Majiagou Formation in the middle Ordos Basin. *Acta Petrolei Sinica*, 26(5): 42–45 (in Chinese with English abstract).

Zhao Weiwei and Wang Baoqing, 2011. Geochemical characteristics of dolomite from 5th Member of the Ordovician Majiagou Formation in Sulige area, Ordos Basin. *Acta Geoscientica Sinica*, 32(6): 681–690 (in Chinese with English abstract).

Zhu Dongya, Meng Qingqiang, Hu Wenxuan and Jin Zhijun, 2012. Deep Cambrian surface karst dolomite reservoir and its alteration by later fluid in Tarim Basin. *Geological Review*, 58 (4): 691–701 (in Chinese with English abstract).

About the first author

LIU Jingdong, male, born in 1984 in Heze City, Shandong province; Ph. D; lecturer in School of Geosciences, China University of Petroleum. He is now interested in the study on reservoir evolution and hydrocarbon reservoir formation. E-mail: ljd840911@126.com; phone: 15865321286.